A NEW PARADIGM FOR GAMMA RAY BURSTS: LONG TERM ACCRETION RATE MODULATION BY AN EXTERNAL ACCRETION DISK

J. K. CANNIZZO[1,2], N. GEHRELS[2]
Draft version May 26, 2009

ABSTRACT

We present a new way of looking at the very long term evolution of GRBs in which the disk of material surrounding the putative black hole powering the GRB jet modulates the mass flow, and hence the efficacy of the process that extracts rotational energy from the black hole and inner accretion disk. The pre-*Swift* paradigm of achromatic, shallow-to-steep "breaks" in the long term GRB light curves has not been borne out by detailed *Swift* data amassed in the past several years. We argue that, given the initial existence of a fall-back disk near the progenitor, an unavoidable consequence will be the formation of an "external disk" whose outer edge continually moves to larger radii due to angular momentum transport and lack of a confining torque. The mass reservoir at large radii moves outward with time and gives a natural power law decay to the GRB light curves. In this model, the different canonical power law decay segments in the GRB identified by Zhang et al. and Nousek et al. represent different physical states of the accretion disk. We identify a physical disk state with each power law segment.

Subject headings: gamma rays: bursts

1. INTRODUCTION

Gamma-Ray Bursts (GRBs) are thought to be energetic events heralding the formation of black holes (BHs): the explosion of a massive star at cosmological distances gives rise to a long GRB, or two neutron stars coalesce to make a short GRB. (For a recent review of GRBs, see Gehrels, Ramirez-Ruiz, & Fox 2009.) To see a GRB at all, our line-of-sight must lie close to the BH angular momentum vector. A jet is launched toward the observer as the BH forms. The initial Lorentz factor of material in the jet $\sim 10^2 - 10^3$ is large enough so that the observer only sees the central portion of the jet, due to relativistic beaming. The transition from "spherical" to "jet-like" expansion of the GRB ejecta is the basis of the current framework within which the analysis of GRB light curves is carried out (Rhoads 1997, 1999; Sari, Piran, & Halpern 1999). Parts of the jet further away from the symmetry axis are initially invisible to the observer, hence the expansion is indistinguishable from that of of a relativistically expanding sphere. Eventually interaction with the circumstellar medium reduces the Lorentz factor until the edges of the jet are visible, after which the decay of the GRB afterglow light curves becomes more rapid. This fundamental property of the decay relies only on special relativity and is not specific to any one wavelength so these theoretical decays should have a similar, strong "break" from shallow to steep across all wavebands, hence the designation "achromatic break".

Frail et al. (2001) studied the decay properties of 17 pre-*Swift* GRBs with redshifts. By analyzing the multiwavelength decay properties, they were able to determine putative break times, which, when combined with distances and isotropic-equivalent GRB energies, allowed a correction to the true, beaming-corrected energy. Frail et al. (2001, see their Fig. 2) show how a spread in isotropic energies between $\sim 10^{52}$ and $\sim 10^{54}$ erg for their sample is considerably reduced down to a standard, geometry-corrected energy centered at $\sim 3 \times 10^{50}$

erg. A detailed examination of the data entering into their study (see their Table 1) shows the sparse coverage of many of the light curves and underscores the difficulty in reliably assigning break times[3]. An updated study along the same lines as Frail et al. (2001) by Bloom, Frail, & Kulkarni (2003) contains a somewhat larger sample – 28 GRBs with redshifts. We should emphasize that we do not argue against the need for beaming; clearly energies as large as $\sim 10^{54}$ erg are problematic, given that $M_\odot c^2 = 1.8 \times 10^{54}$ erg. It is important to distinguish, however, between a time-variable relativistic beaming, and geometric beaming. In this work we adopt a time-constant geometric beaming factor $f_{\rm beam} = 3 \times 10^{-3}$ to convert from isotropic energy to true energy. The question of interest to us is whether the very long term decay in the flux from GRBs, particular the X-ray flux, is due to the deceleration of a jet, or a decreasing mass supply rate onto the central engine.

It was anticipated that *Swift* (Gehrels et al. 2004) would provide good examples of shallow-to-steep achromatic decays. After $\gtrsim 400$ *Swift* GRBs, and now a total of > 170 redshifts for all GRBs (41 for pre-*Swift* GRBs), this has not turned out to be the case. In spite of many GRBs with exquisite wavelength coverage, observed over many $e-$foldings of decay in flux, there is only one GRB in the *Swift* era perhaps showing an achromatic break, seen in X-ray and optical (GRB060206 - Curran et al. 2007) and a small number with candidate jet-breaks (Blustin et al. 2006, Stanek et al. 2007, Dai et al. 2007, Willingale et al. 2007, Kocevski & Butler 2008); the overwhelming majority do not show one (e.g., Oates et al. 2007; Racusin et al. 2008; Liang et al. 2008). Liang et al. (2008) present a thorough investigation of *Swift* XRT and optical jet break candidates. They note that "It is fair to conclude that we *still* have not found a textbook version of a jet break after many years of intense observational campaigns."

Zhang et al. (2006, see their Fig. 1; also Nousek et al. 2006, see their Fig. 3) present a simple schematic for the de-

[1] CRESST/Joint Center for Astrophysics, University of Maryland, Baltimore County, Baltimore, MD 21250, John.K.Cannizzo@nasa.gov

[2] NASA-Goddard Space Flight Center, Greenbelt, MD 20771, gehrels@milkyway.gsfc.nasa.gov

[3] The data used by Frail et al., as well as that for all GRBs, is viewable at http://grblog.org/grblog.php
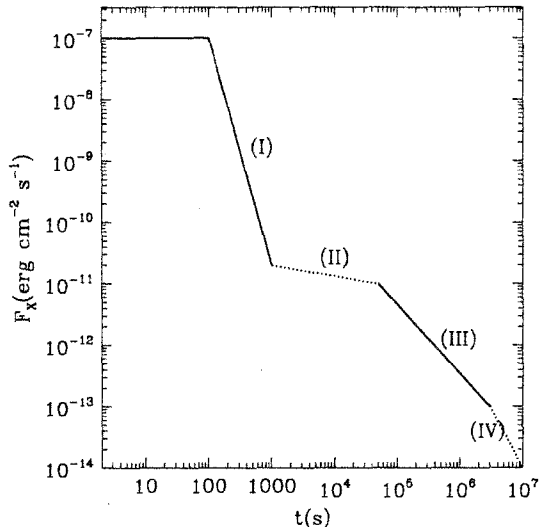
FIG. 1.— A schematic representation of the X-ray decay of a *Swift* GRB as seen with XRT, based on the Zhang et al. (2006) idealization and GRB 060729 from Willingale et al. (2007, see their Fig. 10). To account for cosmological time dilation for a given GRB, the x—axis needs to be shortened by a factor $1 + z$.

caying GRB light curve as seen by the XRT on *Swift*. The decay is traditionally shown in $\log F - \log t$. There are four basic power-law decay ($F \propto t^{-\alpha}$) regimes: (I) $\alpha_I \simeq 3$ out to $10^2 - 10^3$ s, (II) $\alpha_{II} \simeq 0.5$ out to $10^3 - 10^4$ s, (III) $\alpha_{III} \simeq 1.2$ out to $10^4 - 10^5$ s, and (IV) $\alpha_{IV} \simeq 2$ at late times. The general picture given in Zhang et al. based on a handful of case studies from early *Swift* XRT results has been borne out by studies relying on a much larger sample (e.g., O'Brien et al. 2006, Ghisellini et al. 2009). In addition one also frequently sees flares within segment II (Burrows, et al. 2005; for possible explanations see Perna, Armitage, & Zhang 2006, Lazzati, Perna, & Begelman 2008), which are beyond the scope of this work. Figure 1 shows a schematic reproduction of the idealized Zhang et al. light curve, with realistic numbers for the XRT flux. The conversion from the XRT flux values to a beaming-corrected luminosity is given by $L_{\mathrm{XRT}} = 4\pi d_L^2 f_{\mathrm{beam}} F_{\mathrm{XRT}}$, where d_L is the luminosity distance.

In this work we present a framework based on the long term evolution of a transient accretion disk formed out of some small fraction of the progenitor to account for segments II, III, and IV. (Segment I is too steep to be accounted for in our formalism.) The flatness of segment II arises from the transient adjustment of a small amount of gas into an accretion disk, the segment III decay is consistent with the self-similar decay of a disk without a confining external torque, and the increase in slope in segment IV would be caused by the onset of significant disk evaporation (or by the late-time accretion from a super-Eddington slim disk). The consistency of the theoretical decay with segment III argues for a direct association, and the fact that it takes some time for an arbitrary initial mass profile to adjust into a disk leads to the transient interval (segment II).

This work applies mainly to the commonly observed "long" GRBs which are believed to be due to the core collapse of a massive, high angular momentum progenitor, leading to the formation of black hole — the "collapsar" model (Woosley 1993; MacFadyen & Woosley 1999; Woosley & Bloom 2006;

Nagataki et al. 2007). There follows a period of electromagnetic extraction of energy from the BH which powers a collimated jet. For $\sim 10^2 - 10^3$s following the phase of prompt GRB emission, $\sim 0.1 M_\odot$ of bound matter from the disrupted progenitor star returns to the BH vicinity due to conservation of angular momentum. Kumar, Narayan, & Johnson (2008ab) attempt to explain the long-term *Swift* X-ray light curves in terms of various phases of an accretion model. They argue that the rapid accretion of the outer half of the core of the progenitor, possessing a density profile that drops steeply with radius, can lead to the initial, rapid decay. For the flat segment (II) they discuss briefly the idea of having a small accretion disk viscosity, but ultimately discard this explanation in favor of prolonged fall-back of gas from the envelope of the progenitor at larger radii, which they argue can supply matter to the central engine at a near-constant rate, or a rate that decreases slightly with time. Kumar et al. (2008a) also present analytic time dependent solutions for an accretion disk in an ADAF-like state (ADAF = advection dominated accretion flow) and show that, for a radial mass profile $\dot{M}(r) \propto r^s$, the decay law would be $\alpha_{III} = 4(s + 1)/3$. For $s = 0$, i.e., no wind mass-loss from the disk, the decay is close to the Zhang et al. (2006) value. Under the assumptions of core fall-back for segment I and envelope fall-back for segment II, Kumar et al. (2008b) place constraints on the progenitor core and envelope radii, their density profiles, and the pre-SN rotation rates of the core and envelope, normalized to their Keplerian values.

In Section 2 we discuss the physics of accretion disks, both steady state and time dependent. Section 3 presents a scenario for the overall, long term evolution of the external accretion disk, section 4 presents a discussion, section 5 discusses the implications of the theory, and section 6 sums up.

2. ACCRETION DISK PHYSICS

Most of the previous discussion of GRB fall-back disks has failed to recognize one unavoidable aspect of their existence: namely, their outer edge moves outward with time, carrying with it mass and angular momentum. (Notable exceptions are Kumar et al. [2008ab].) One can make simple arguments about the perturbation accretion time scale near the central engine based on physical conditions there, but the outer portions are causally linked to the inner regions through angular momentum transport, and it is these outlying regions that set the long-term accretion disk time scales.

The physical agent responsible for angular momentum transport and turbulent dissipation of energy is now believed to be the magneto-rotational instability (MRI) or Balbus-Hawley instability (Balbus & Hawley 1998) which involves the shearing amplification of a weak seed magnetic field. The general process of angular momentum transport and energy dissipation in accretion disks is still commonly referred to as "viscosity". Balbus & Papaloizou (1999) show a foundation for the dynamical "α" view of accretion disks (Shakura & Sunyaev 1973) within the MRI.

Extensive study of accretion disks in interacting binaries has guided thought on accretion disks in other types of systems, such as around BHs in AGNs. For instance, the best constraint we have of the magnitude of the α parameter comes from a detailed study of the rate of decay of dwarf nova outbursts (Smak 1984), and the values obtained for ionized gas $\alpha \simeq 0.1 - 0.2$ have been carried over to accretion disks in other systems.

One aspect of accretion disks which is quite different for isolated BHs is the lack of a constraint on the outer radius.

The sudden introduction of an annulus of gas near a central mass leads to a process of smearing of the matter into a broadened ring. The ring spreads both to smaller and larger radii in response to outward transport of angular momentum. As mass drains from the inner edge, an ever smaller amount of material moves to larger and larger radii. Pringle (1974) studied "external accretion disks" in which matter initially in a torus spreads both to smaller and larger radii. The class of solutions he considered of relevance to this work is that for disks with constant total angular momentum and decreasing mass. Pringle (1991) generalized his earlier results.

By writing the equations for mass continuity and angular momentum transport in cylindrical coordinates, assuming Keplerian rotation $\Omega_K^2 = GM_{\rm BH}r^{-3}$ and a thin accretion disk, and integrating over the vertical thickness of the accretion disk, one arrives at an equation for the evolution of the surface density $\Sigma = 2\rho h$, where ρ is the density and h the disk semithickness (actually pressure scale height),

$$\frac{\partial \Sigma}{\partial t} = \frac{3}{r}\frac{\partial}{\partial r}\left[r^{1/2}\frac{\partial}{\partial r}\left(\nu\Sigma r^{1/2}\right)\right]. \qquad (1)$$

The kinematic viscosity coefficient

$$\nu = \frac{2\alpha P}{3\Omega_K\rho}, \qquad (2)$$

where P is the pressure and α is the Shakura-Sunyaev parametrization of the angular momentum transport and heating (Shakura & Sunyaev 1973). Debate persisted over many years as whether the viscosity should scale with the total pressure or gas pressure. A scaling with the total pressure leads to a strong dynamical instability in regions where $P_{\rm rad} > P_{\rm gas}$ — the Lightman-Eardley instability (Lightman & Eardley 1974) — which manifests itself as a limit cycle operating in the inner, radiation pressure dominated portions of the disk (e.g., Cannizzo 1997). However, the fact that X-ray binaries with very high rates of accretion, such as Sco X-1, often have perfectly stable light curves leads one to conclude that the Lightman-Eardley instability is probably the artifact of an incorrect assumption for thin disks, namely $\nu \propto P_{\rm total}$ (Done, Gierliński, & Kubota 2007). With the advent of the MRI, detailed MHD calculations show that the saturation limit of the instability depends on the magnetic energy density reaching a limit that may depend on surface density rather than pressure (e.g., Hirose, Krolik, & Blaes 2009). Hirose et al. find not only that radiation dominated disks are thermally stable, but that fluctuations in magnetic field strength causally precede those in pressure (both radiation and gas). Hirose et al. suggest adopting Σ as the relevant independent variable.

The MRI couples linearly to the Keplerian shear in the disk and dissipates energy through turbulent transport. In formulating the steady state equations for the radial profile of accretion disk structure, one begins by equating a heating function

$$Q_{\rm vis}^- = \frac{9}{8}\nu\Sigma\Omega_K^2 \qquad (3)$$

with a cooling function

$$Q_{\rm rad}^- = \frac{4}{3}\frac{ac}{\kappa\rho}\frac{T^4}{h}, \qquad (4)$$

assuming an optically thick vertical structure with energy transported by radiative diffusion. The vertically integrated stress provides the total radiated flux (assuming no radial advection of energy)

$$Q = \sigma T_{\rm eff}^4 = \frac{3}{8\pi}\dot{M}\Omega_K^2. \qquad (5)$$

Finally, the condition of vertical hydrostatic equilibrium in the disk gives

$$\frac{P_{\rm total}}{\rho} = \Omega_K^2 h^2. \qquad (6)$$

2.1. Blandford-Znajek Coupling to the Inner Disk

After a period of equilibration and expansion, the external disk may span many decades in radius — from $\sim 10^7$ to $\sim 10^{11}$ cm. The physical state of the disk is expected to vary enormously as one progresses from small to large radii. In terms of mediating the flow of mass down onto the central engine, the similarity solutions just discussed rely on the physical state of the outer disk. The physical state of the inner disk determines the strength of the Blandford-Znajek (BZ) process (Blandford & Znajek 1977) that extracts rotational energy from the central BH. Ghosh & Abramowicz (1997) examined the dependence of the strength of the BZ mechanism on physical conditions in the inner disk. The energy density of the magnetic field entrained within the disk sets the BZ luminosity, and insofar as the saturation limit is set by equipartition with the pressure, the maximum pressure $p_{\rm max}$ is of relevance.

Livio, Ogilvie, & Pringle (1999) investigated the role of the BZ mechanism in powering outflows and found that if the magnetic field threading the inner disk does not differ significantly in strength from that threading the black hole, the electromagnetic output from the inner disk regions should dominate over that from the hole. In simple terms, the disk is more efficient at holding and accelerating the magnetic field because its magnetic diffusivity is much less than that of the BH.

However, more recent works using sophisticated GRMHD codes to follow the detailed magnetohydrodynamic launching of flows from the very inner disk find them to be highly efficient in terms of tapping the available supply of rest mass-energy in the disk. (McKinney & Narayan 2007ab; Krolik, Hawley, & Hirose 2007). McKinney & Narayan (2007a) note that previous simple estimates of the BH and disk failed to take into account the conversion of EM power into thermal and material power in the corona and disk wind (Ghosh & Abramowicz 1997, Livio, Ogilvie, & Pringle 1999) and so may have seriously overestimated the power from the disk, in which case the BH power may dominate. Krolik, Hawley, & Hirose (2007, see their Table 1) find high efficiencies $\epsilon_{\rm beam}$ for the jet power, measured either in terms of mass, radiative energy, or EM energy, normalized to the rest mass-energy accretion in the disk $\dot{M}c^2$. Their radiative efficiency values (which they denote $\eta_{\rm NT}$) increase with a/M, ranging from 0.057 for $a/M = 0$ up to 0.264 for $a/M = 0.99$. The efficiencies may increase with time due to BH spin-up. These workers find the jet to be Poynting flux dominated near the BH spin axis, giving strength to the idea of a lightweight jet that responds quickly to changes in $\dot{M}$ in the inner disk. In this work we adopt $\epsilon_{\rm beam} = 0.1$ as a fiducial value relating the jet energy production as seen in X-rays to the accretion rest mass-energy within the main body of the accretion disk.

Initially the accretion rate can approach $\sim 1 M_\odot$ s^{-1}, i.e., super-Eddington by a factor $\sim 10^{14}$. One might question whether an accretion disk description is fully applicable. Studies of the inner disk at these very early times find that the temperatures and densities are so large that the cooling is by neutrino emission (Narayan, Piran, & Kumar 2001, Kohri & Mineshige 2002, Kohri, Narayan, & Piran 2005, Chen & Be-

loborodov 2007). Chen & Beloborodov (2007) show that for a BH with high spin $a \sim 1$ a neutrino cooling dominated disk transitions to an advective disk at $\sim 10^{-3} - 10^{-2} M_\odot$ s^{-1}. Kohri & Mineshige (2002, see their Fig. 1) detail the different physical regimes of these disks. The cooling function

$$Q^- = Q^-_{\rm rad} + Q^-_{\rm adv} + Q^-_\nu, \qquad (7)$$

where Q^-_ν is the neutrino cooling.

2.2. Eddington Luminosity and Accretion Rate

For the GRB depicted schematically in Fig. 1, $z = 0.54$ and $d_L = 3.1$ Gpc. The inferred, beaming-corrected X-ray luminosity corresponding to the earliest time we seek to address, namely the onset of segment II, would be $L_{\rm II} = 4\pi d_L^2 f_{\rm beam} F_{\rm XRT, II} \simeq 3 \times 10^{43}$ erg s^{-1}, where we used $F_{\rm XRT, II} = 10^{-11}$ erg cm^{-2} s^{-1} (Grupe et al. 2007; see their Fig. 4) and $f_{\rm beam} = 3 \times 10^{-3}$. The isotropic-equivalent X-ray plateau luminosity for this GRB, $\sim 10^{46}$ erg s^{-1}, is in about the middle (logarithmically) of the range 10^{44} erg s$^{-1} \lesssim 4\pi d_L^2 F_{\rm XRT, II} \lesssim 10^{48}$ erg s^{-1} shown in Dainotti et al. (2008; see their Figs. 1 and 2). Adopting $\epsilon_{\rm beam} = 0.1$, the geometry-corrected luminosity translates into a rate of accretion in the inner disk $L_{\rm II}/(\epsilon_{\rm beam} c^2) \simeq 5.3 \times 10^{-3} M_\odot$ yr^{-1}. In the conventional view, for rates of accretion larger than the Eddington rate

$$L_E = \frac{4\pi G M_{\rm BH} c}{\kappa_{\rm es}} \simeq 1.25 \times 10^{39} (M_{\rm BH}/10 M_\odot)\ {\rm erg\ s}^{-1} \qquad (8)$$

radiation pressure impedes the accretion process (see below, however, for the possibility of a slim disk). The Eddington accretion rate depends on radius, through the local efficiency with which gravitational energy is radiated $\epsilon_{\rm acc}(r) \equiv G M_{\rm BH}/(r c^2)$. The locally defined Eddington accretion rate $\dot{M}_E(r)$ is related to the Eddington luminosity via

$$L_E = \epsilon_{\rm acc}(r) \dot{M}_E(r) c^2. \qquad (9)$$

Thus $\epsilon_{\rm acc}(r) \propto r^{-1}$ and $\dot{M}_E(r) \propto r$, varying from $1.3 \times 10^{-7} M_\odot$ yr^{-1} in the inner disk $6 G M_{\rm BH}/c^2$ to $1.5 \times 10^{-3} M_\odot$ yr^{-1} at 10^{11} cm. Therefore in the region of interest to us in this study, namely the outermost part of the disk, the rate would only be locally super-Eddington by a factor ~ 3 at this early time.

The preceding discussion was based on the standard assumption of solar composition material, which is almost certainly not the case here. The fall-back matter comprising the disk would be expected to be dominated by $r-$processed material - Ni, Si, and Fe group elements. Calculations of the Eddington limit for such material indicate a potential suppression of the standard Eddington value by up to about three orders of magnitude due to increased opacity from lines (e.g., Fryer, Colgate, & Pinto 1999). However, this applies mainly to much lower temperatures than those discussed in the next section.

2.3. Steady State Physics

2.3.1. Standard Thin Disk

Cannizzo & Reiff (1992) present general Shakura-Sunyaev scalings for disks with arbitrary opacity law. For optically thick disks for which $\nu \propto P_{\rm gas}$, $\kappa = \kappa_{\rm es} = 0.2(1 + X) = 0.2$ cm^2 g^{-1} (no hydrogen), and mean molecular weight $\mu = 16$ (appropriate for the expected for mixture of alpha elements

- predominantly ^{56}N, ^{28}Si, ^{16}O, and ^{12}C - Fryer, Colgate, & Pinto 1999), the surface density

$$\Sigma = 2.84 \times 10^7\ {\rm g\ cm}^{-2}\ r_{11}^{-3/5}\ m_{\rm BH,\ 1}^{1/5}\ \alpha_{-1}^{-4/5}\ \dot{m}_{-2}^{3/5}, \qquad (10)$$

where $r_{11} = r/10^{11}$ cm, $m_{\rm BH,\ 1} = M_{\rm BH}/10 M_\odot$, $\alpha_{-1} = \alpha/0.1$, $\dot{m}_{-2} = \dot{M}/10^{-2} M_\odot$ yr^{-1}. (In the region of interest for this study $\dot{m}_{-2} \simeq 0.01 - 1$.) The midplane temperature

$$T = 7.83 \times 10^6\ {\rm K}\ r_{11}^{-9/10}\ m_{\rm BH,\ 1}^{3/10}\ \alpha_{-1}^{-1/5}\ \dot{m}_{-2}^{2/5}. \qquad (11)$$

The disk temperature is less than the virial temperature

$$T_{\rm virial} = \frac{1}{6} \frac{\mu}{\mathcal{R}} \frac{GM}{r} = 4.26 \times 10^8\ {\rm K}\ r_{11}^{-1}\ m_{\rm BH,\ 1}. \qquad (12)$$

The only assumptions needed up to this point are $Q^+ = Q^- = Q$. To obtain the disk scale height and density, we now specify $P = P_{\rm gas}$. This yields a pressure scale height to disk radius ratio

$$\frac{h}{r} = 0.055\ r_{11}^{1/20}\ m_{\rm BH,\ 1}^{-7/20}\ \alpha_{-1}^{-1/10}\ \dot{m}_{-2}^{1/5}, \qquad (13)$$

a density

$$\rho = 2.57 \times 10^{-3}\ {\rm g\ cm}^{-3}\ r_{11}^{-33/20}\ m_{\rm BH,\ 1}^{11/20}\ \alpha_{-1}^{-7/10}\ \dot{m}_{-2}^{2/5}, \qquad (14)$$

and self-gravity to central object gravity

$$\frac{g_s}{g_c} = \frac{2\pi G \Sigma}{\Omega_K^2 h} = 1.62 \times 10^{-3}\ r_{11}^{27/20}\ m_{\rm BH,\ 1}^{-9/20}\ \alpha_{-1}^{-7/10}\ \dot{m}_{-2}^{2/5}. \qquad (15)$$

The radiation pressure to gas pressure ratio

$$\frac{P_{\rm rad}}{P_{\rm gas}} = 91\ r_{11}^{-21/20}\ m_{\rm BH,\ 1}^{7/20}\ \alpha_{-1}^{1/10}\ \dot{m}_{-2}^{4/5} \qquad (16)$$

exceeds unity, therefore the pressure scale height, which was predicated upon $P = P_{\rm gas}$, should be increased by a factor $\sqrt{92} \approx 10$ to $h/r \simeq 0.5$ because of hydrostatic equilibrium. Note that because we adopt $\nu \propto P_{\rm gas}$, the fact that $P_{\rm rad} > P_{\rm gas}$ is not problematic in itself as long as $h/r << 1$. However, the fact that $h/r \simeq 0.5$ begins to be problematic.

As a last consistency check, the ratio of the flux of radially advected energy $(\dot{M}/2\pi r^2) c_s^2$ to vertically transported energy

$$\frac{Q^-_{\rm adv}}{Q^-_{\rm rad}} = \frac{3}{16\pi} \frac{\kappa_{\rm es} \mathcal{R}}{ac\mu} \frac{\dot{M}\Sigma}{r^2 T^3} \qquad (17)$$

$$= 1.02 \times 10^{-3}\ r_{11}^{1/10}\ m_{\rm BH,\ 1}^{-7/10}\ \alpha_{-1}^{-1/5}\ \dot{m}_{-2}^{2/5}. \qquad (18)$$

In summary, the standard model is marginally self-consistent for representative values in the outer disk $r_{11} \simeq \dot{m}_{-2} \simeq 1$.

Note that for $m_{\rm BH,\ 1} = r_{11} = 1$, we have $\epsilon_{\rm acc}(r) \simeq 1.5 \times 10^{-5}$ and $\dot{M}_E(r) \simeq 1.5 \times 10^{-3} M_\odot$ yr^{-1}. A value $\dot{m}_{-2} \simeq 0.5$ (determined from $L_{\rm II}$) at $r_{11} = 1$ would be locally super-Eddington only by a factor ~ 3, but by larger factors at smaller radii since $\dot{M}_E(r) \propto r$. As noted earlier, the true super-Eddington factors could be greater for the $r-$processed gas, although for $T \simeq 10^7$ K the opacity is basically electron scattering, which is actually suppressed due to the fact that the hydrogen fraction $X = 0$, and $\kappa_{\rm es} \propto (1 + X)$. At smaller radii the standard model would become quite problematic due to $P_{\rm rad}/P_{\rm gas} >> 1$ leading to $h/r \gtrsim 1$, and $\dot{M}/\dot{M}_E(r) >> 1$. Although a detailed description of the disk at smaller radii is not of primary relevance to this work, we briefly look at two formalisms of potential interest.

2.3.2. *Super-Eddington Slim Disk*

For disks with accretion rates of order Eddington, the sizable radial gradients demand the introduction of a radial advective energy transport term (Abramowicz et al. 1988, Chen et al. 1995; Kato, Fukue, & Mineshige 1998). The cooling function is now written

$$Q^- = Q^-_{\rm rad} + Q^-_{\rm adv}, \tag{19}$$

where the advective transport

$$Q^-_{\rm adv} = \Sigma T v_r \frac{ds}{dr}, \tag{20}$$

and s is the entropy per particle. This can be written as

$$Q^-_{\rm adv} = \Sigma v_r \frac{p}{\rho} \zeta, \tag{21}$$

where ζ is a logarithmic derivative involving s that is of order unity (Chen et al. 1995), or

$$Q^-_{\rm adv} = \frac{\dot{M}}{2\pi r^2} c_s^2, \tag{22}$$

where $c_s^2 = (3/2)GM/r$. The anticipated accretion rate $\sim 3\dot{M}_{\rm E}(r)$ at $r_{11} = 1$ places the accretion disk model on the upper stable branch of slim disk solutions (Abramowicz et al. 1988, see their Fig. 4) where radiation pressure dominates (Kato, Fukue, & Mineshige 1998, see their section 10.1.1). Solving the disk parameters for $P = P_{\rm rad}$ gives

$$\Sigma = \frac{2\dot{M}}{9\pi r^2 \Omega_K \alpha} \tag{23}$$

$$= 3.87 \times 10^4 \text{ g cm}^{-2} \, r_{11}^{-1/2} \, m_{\rm BH,\,1}^{-1/2} \, \alpha_{-1}^{-1} \, \dot{m}_{-2}, \tag{24}$$

$$T = \left(\frac{3\Omega_K \dot{M}}{4\pi a r \alpha} \right)^{1/4} \tag{25}$$

$$= 1.23 \times 10^6 \text{ K } r_{11}^{-5/8} \, m_{\rm BH,\,1}^{1/8} \, \alpha_{-1}^{-1/4} \, \dot{m}_{-2}^{1/4}, \tag{26}$$

$$\frac{h}{r} = \sqrt{\frac{3}{4}} = 0.866, \tag{27}$$

$$\rho = 2.23 \times 10^{-7} \text{ g cm}^{-3} \, r_{11}^{-3/2} \, m_{\rm BH,\,1}^{-1/2} \, \alpha_{-1}^{-1} \, \dot{m}_{-2}, \tag{28}$$

$$\frac{P_{\rm rad}}{P_{\rm gas}} = 4.05 \times 10^3 \, r_{11}^{-3/8} \, m_{\rm BH,\,1}^{7/8} \, \alpha_{-1}^{1/4} \, \dot{m}_{-2}^{-1/4}, \tag{29}$$

and

$$\frac{Q^-_{\rm adv}}{Q^-_{\rm rad}} = \frac{\kappa_{\rm es}\dot{M}}{12\pi cr} = \frac{1}{3}\frac{\dot{M}}{\dot{M}_E(r)} = 1.12 \, r_{11}^{-1} \, \dot{m}_{-2}. \tag{30}$$

Thus the starting assumptions $P_{\rm rad} > P_{\rm gas}$ and $Q^-_{\rm adv} > Q^-_{\rm rad}$ are validated.

2.3.3. *Marginally Eddington Disk with $P = P_{\rm rad}$*

In view of the super-Eddington accretion rates, another possibility worth investigating is a disk in which strong mass outflow due to radiation pressure driven winds occurs as the local accretion rate begins to exceed $\dot{M}_E$. Since the aspect ratio

$$\frac{h}{r} \simeq \frac{\dot{M}(r)}{\dot{M}_E(r)} \tag{31}$$

(Shakura & Sunyaev 1973), the maintenance of a disk bordering on being Eddington at all radii would enforce $h/r = 1$. The disk would be non-steady state,

$$\dot{M}(r) = \frac{32\pi}{3} \frac{c}{\kappa_{\rm es}} r, \tag{32}$$

and strong winds would be generated at all radii. Solving for the disk variables with $P = P_{\rm rad}$ and $h/r = 1$ yields

$$\Sigma = \frac{16}{3\alpha\Omega_K} \frac{c}{\kappa_{\rm es} r} \tag{33}$$

$$= 6.94 \times 10^4 \text{ g cm}^{-2} \, r_{11}^{1/2} \, m_{\rm BH,\,1}^{-1/2} \, \alpha_{-1}^{-1}, \tag{34}$$

$$T = \left(\frac{3}{2} \frac{r\Omega_K^2}{a} \Sigma \right)^{1/4} \tag{35}$$

$$= 1.16 \times 10^6 \text{ K } r_{11}^{-3/8} \, m_{\rm BH,\,1}^{1/8} \, \alpha_{-1}^{-1/4}, \tag{36}$$

$$\frac{h}{r} = 1, \tag{37}$$

$$\rho = 3.47 \times 10^{-7} \text{ g cm}^{-3} \, r_{11}^{-1/2} \, m_{\rm BH,\,1}^{-1/2} \, \alpha_{-1}^{-1}, \tag{38}$$

and

$$\frac{P_{\rm rad}}{P_{\rm gas}} = 2.20 \times 10^3 \, r_{11}^{-5/8} \, m_{\rm BH,\,1}^{7/8} \, \alpha_{-1}^{1/4}. \tag{39}$$

Since there is no dependence on accretion rate, this state would persist, in theory, until $\dot{M}$ dropped below $\dot{M}_E$ at the outer edge. An annular region with constant $\dot{M}(r)$ would then begin to propagate to smaller radii. This appears at first glance to raise the intriguing possibility of applying this long period of constant accretion onto the central engine to explain the plateau phase of the light curve shown in Fig. 1 (segment II). If each annulus in the disk emits at roughly its local Eddington limit, an integration over the disk shows that the total accretion luminosity can exceed L_E by a factor $\sim \ln(\dot{M}[r_{\rm outer}]/\dot{M}_E[r_{\rm inner}])$ (Shakura & Sunyaev 1973; Begelman, King, & Pringle 2006) which would have a value ~ 10 in the current application. However, the inferred GRB segment II luminosity $L_{\rm II} \simeq 3 \times 10^{43}$ erg s$^{-1}(f_{\rm beam}/3 \times 10^{-3})$ greatly exceeds even this enhanced Eddington value $\sim 10 \times L_E(10M_\odot) \sim 10^{40}$ erg s^{-1}, unless the beaming factor were orders of magnitude smaller than the value 3×10^{-3} we take in this study. Such a tightly collimated flow would not be expected from an Eddington outflow.

2.4. *Time Dependent Behavior of External Disks*

Pringle (1974, 1991) presented exact self-similar solutions for the time dependent behavior of disks with a free outer boundary for the viscosity parameterization

$$\nu = \nu_0 \left(\frac{\Sigma}{\Sigma_0} \right)^m \left(\frac{r}{r_0} \right)^n. \tag{40}$$

Of interest are the class of solutions for which the disk total angular momentum is constant.

2.4.1. *Standard Model*

For the simplest case — gas pressure and electron scattering opacity — one may combine eqns. (2)-(4) to find

$$\nu = Cr\Sigma^{2/3}, \tag{41}$$

where

$$C = \alpha^{4/3} \left(\frac{k_B}{\mu m_p}\right)^{4/3} \left(\frac{\kappa_{\rm es}}{12acGM_{\rm BH}}\right)^{1/3}. \quad (42)$$

This is in the form considered by Pringle (1991) for $m = 2/3$ and $n = 1$. The solution is

$$\frac{\Sigma(r,t)}{\Sigma_0} = \left(\frac{t}{t_0}\right)^{-15/16} f\left[\left(\frac{r}{r_0}\right)\left(\frac{t}{t_0}\right)^{-3/8}\right]. \quad (43)$$

where

$$f(u) = (28)^{-3/2} u^{-3/5} \left(1 - u^{7/5}\right)^{3/2} \quad (44)$$

(Cannizzo, Lee, & Goodman 1990), which can be verified by substitution into eqn. (1). The dimensional scalings Σ_0, r_0, and t_0 satisfy

$$t_0 = r_0 C^{-1} \Sigma_0^{-2/3}. \quad (45)$$

The solution given in eqn. (43) extends out to $u = 1$, so that the spreading of the outer edge varies as $(r/r_0) = (t/t_0)^{3/8}$. The right hand side of eqn. (43) multiplies the Σ solution from eqn. (10). The total disk angular momentum is constant, and the disk mass decreases as

$$M_d(t) = (28)^{-3/2}\frac{4\pi}{7}r_0^2\Sigma_0 \left(\frac{t}{t_0}\right)^{-3/16}, \quad (46)$$

and therefore the available accretion luminosity $L_d(t) \propto \dot{M}_d \propto t^{-19/16}$.

2.4.2. *Super-Eddington Slim Disk*

In this model

$$\nu = C_{\rm adv} r^{1/2}, \quad (47)$$

where

$$C_{\rm adv} = \frac{9}{4}\alpha(GM_{\rm BH})^{1/2}. \quad (48)$$

For $m = 0$ and $n = 1/2$ the solution from Pringle (1991; see his eqn. [3.2.8]) is

$$\frac{\Sigma(r,t)}{\Sigma_0} = \left(\frac{r}{r_0}\right)^{-1/2}\left(\frac{t}{t_0}\right)^{-4/3}(1 - ku^b)^a, \quad (49)$$

where $u = (r/r_0)^{1/2}(t/t_0)^{-1/3}$, $k = m(4m + 4 - 2n)^{-1}(5m + 4 - 2n)^{-1} \propto m = 0$, $a = 1/m \to \infty$, and $b = 3$. Euler's formula

$$\lim_{\mu \to \infty}\left(1 + \frac{x}{\mu}\right)^\mu = e^x \quad (50)$$

enables us to recast Σ as

$$\frac{\Sigma}{\Sigma_0} = \left(\frac{r}{r_0}\right)^{-1/2}\left(\frac{t}{t_0}\right)^{-4/3}\exp\left[-\frac{1}{9}\left(\frac{r}{r_0}\right)^{3/2}\left(\frac{t}{t_0}\right)^{-1}\right]. \quad (51)$$

Integration of $2\pi r dr \Sigma(r,t)$ for the disk mass gives

$$M_d(t) = 12\pi r_0^2 \left(\frac{t}{t_0}\right)^{-1/3}\Sigma_0\left(1 - \exp\left[-\frac{1}{9}\left(\frac{t}{t_0}\right)^{-1}\right]\right). \quad (52)$$

For $t \ll t_0/9$, the exp term will go to zero. Hence one has $M_d \propto t^{-1/3}$ and therefore $L_d \propto t^{-4/3}$, in agreement with Kumar et al. (2008a) for $s = 0$. For late times $t \gg t_0/9$,

expanding $\exp(-x)$ as $1 - x$ and combining the t dependencies gives a steeper decay, $L_d \propto t^{-7/3}$. The dividing point $t_{\rm divide} = t_0/9$ between $L_d \propto t^{-4/3}$ and $L_d \propto t^{-7/3}$ can be evaluated by using the closure relation between $C_{\rm adv}$, r_0, and t_0, yielding

$$t_{\rm divide} = \frac{16}{243}(\alpha\Omega_0)^{-1} = 570\ {\rm s}\ r_{0,\ 11}^{3/2}\ m_{{\rm BH},\ 1}^{-1/2}\ \alpha_{-1}^{-1}, \quad (53)$$

where $\Omega_0 = \Omega_K(r_0)$.

2.4.3. *Irradiation-dominated Disk*

At very late times corresponding to segment IV, which is not always seen, one needs also to consider irradiation-dominated disks. For disks in which the locally defined irradiation temperature $T_{\rm irr} = [L_{\rm acc}/(4\pi\sigma r^2)]^{1/4}$, where $L_{\rm acc} = \epsilon_{\rm acc}\dot{M}c^2$, exceeds the disk midplane temperature, the viscous heating of the disk will be subordinate to irradiational heating. One now finds [4]

$$\nu = C_{\rm irr}r^{4/3}\Sigma^{1/3}, \quad (54)$$

where

$$C_{\rm irr} = \alpha^{4/3}\left(\frac{k_B}{\mu m_p}\right)^{4/3}\left(\frac{4\epsilon_{\rm acc}c^2}{27\sigma G^2 M_{\rm BH}^2}\right)^{1/3}. \quad (55)$$

This is in the form considered by Pringle (1991) for $m = 1/3$ and $n = 4/3$. The solution is

$$\frac{\Sigma(r,t)}{\Sigma_0} = \left(\frac{t}{t_0}\right)^{-5/3} f\left[\left(\frac{r}{r_0}\right)^{1/2}\left(\frac{t}{t_0}\right)^{-1/3}\right], \quad (56)$$

where

$$f(u) = (18)^{-3}u^{-2}\left(1 - u^2\right)^3. \quad (57)$$

The disk mass

$$M_d(t) = (18)^{-3}\frac{\pi}{2}r_0^2\Sigma_0\left(\frac{t}{t_0}\right)^{-1/3}, \quad (58)$$

so the disk luminosity $L_d \propto t^{-4/3}$.

3. GENERAL SCENARIO

We argue that the entire X-ray sequence spanning $> 10^6$ s can be understood in terms of the external accretion disk passing through a sequence of different physical states. We propose that the jet becomes active almost immediately after creation of the BH and the beginning of formation of the fall-back disk. The subsequent decrease in X-ray luminosity is then due to the decreasing mass supply in the inner disk. The current paradigm is that a jet of material launched from the core of the progenitor decelerates as it encounters circumstellar material (Sari et al. 1999; Frail et al. 2001).

In the following discussion of the four Zhang et al. regimes, we adopt GRB 060729 as a specific example due to its very long coverage both in terms of flux decay and time (both span ~ 7 decades — see Grupe et al. 2007 for a detailed study). The light curve (Grupe et al. 2007, see their Fig. 4; Willingale et al. 2007, see their Fig. 10) shows a $0.3 - 10$ keV flux initially at $\sim 3 \times 10^{-7}$ erg cm^{-2} s^{-1} at ~ 100s, decreasing to $\sim 2 \times 10^{-11}$ at $\sim 10^3$s, then down slightly to $\sim 10^{-11}$ by $\sim 5 \times 10^4$s, and finally to $\sim 3 \times 10^{-14}$ at

---

[4] Menou, Perna, & Hernquist (2001, see their Appendix A2) neglect the $\dot{M}$ (and hence Σ) dependence of ν, and therefore effectively derive a similarity solution for a disk with constant irradiation.

$\sim 5 \times 10^6$s. The redshift $z = 0.54$ gives, for the standard cosmology, a luminosity distance $d_L = 3.1$ Gpc, so that $4\pi d_L^2 \simeq 1.15 \times 10^{57}$ cm^2. To take into account cosmological time dilation the long term light curve depicted schematically in Fig. 1 should also be contracted along the x-axis by a factor $1 + z = 1.54$. Adopting a geometric beaming factor $f_{\rm beam} \sim 3 \times 10^{-3}$, a beam efficiency $\epsilon_{\rm beam} = L_{\rm beam}/(\dot{M}c^2) \sim 0.1$, and neglecting the bolometric correction, the plateau flux $F_{\rm XRT,\ II} \simeq 10^{-11}$ erg cm^{-2} s^{-1} translates into an isotropic luminosity $4\pi d_L^2 F_{\rm XRT,\ II} = 1.2 \times 10^{46}$ erg s^{-1}, a beaming corrected luminosity $L_{\rm II} = 3.6 \times 10^{43}$ erg s^{-1}, and a rest mass-energy flux in the disk $\dot{M}c^2 = L_{\rm II}/\epsilon_{\rm beam} = 3.6 \times 10^{44}$ erg s^{-1}, which would not be directly observable presumably due to the advective nature of the inner disk. This value is significantly in excess of the Eddington value $L_E \simeq 1.3 \times 10^{39}(M_{\rm BH}/10 M_\odot)$ erg s^{-1}. It is also important to acknowledge that the very long duration of the plateau for GRB 060729, $\sim 50,000$s, is not typical. Dainotti et al. (2008) find a range between about 10^2s and 10^5s in plateau duration, corrected to the source frame.

Taking $f_{\rm beam} = 3 \times 10^{-3}$ and $\epsilon_{\rm beam} = 0.1$ for entire evolution shown in Fig. 1 (which is probably unrealistic), the amount of matter accreted during each segment is $1.5 \times 10^{-4} M_\odot$ for the prompt emission out to 100s, $5.5 \times 10^{-5} M_\odot$ for segment I, $8.5 \times 10^{-6} M_\odot$ for segment II, $2.4 \times 10^{-5} M_\odot$ for segment III, and $1.7 \times 10^{-6} M_\odot$ for segment IV. It is important to note that these numbers represent the bookkeeping associated with the powering of the jet, which we are assuming produces the X-rays. Given the likelihood of significant mass depletion within the disk, e.g., $\dot{M}(r) \propto r^s$, with s in the range 0 to 1 (Kumar et al. 2008a), the actual total mass available from fall-back could be orders of magnitude larger, $\sim 0.1 - 1 M_\odot$. Given the long term persistence of the external disk, the logarithmic rate of decay for each of the four segments identified by Zhang et al. (2006) must be relatable to different physical regimes the disk passes through during its long period of mass depletion:

3.1. *Segment I: Fall-back Debris*

$\alpha_{\rm I} \simeq 3$ for $10^2 \lesssim t \lesssim 10^3$ s: During this early time the inner disk is being dynamically assembled out of fall-back material, and so the assumptions entering into the similarity solution for the evolution of the external disk are not yet valid. Kumar, Narayan, & Johnson (2008a) considered the evolution of debris from the SN event that disrupts the progenitor and creates the BH and subsequent GRB, and show analytically that the arrival of material onto the BH from the collapse of the outer half of the progenitor core leads to $\dot{M} \sim t^{-3}$. In their model the rapid infall of matter arises because of the steep density profile of the outer core. During this early period of extremely high accretion rate $\gtrsim 10^{10} L_E$ initially, the inner disk may contain regions where the cooling is neutrino-dominated and then advection-dominated. During the early, chaotic phase of fall-back and accretion, the high rate of accretion significantly depletes the amount of material surrounding the BH.

It has been suggested that early in the evolution of the disk self-gravity may play a role (e.g., Perna, Armitage, & Zhang 2006). Therefore it may be possible to account for this early evolution purely within the confines of an accretion disk formalism, through considering self-gravitating disks (J. Pringle, 2008, private communication), although it is not clear a priori whether such a steep decay law can be obtained. If there is

still substantial material at small radii left over from the immediate post-GRB accretion (MacFadyen & Woosley 1999), it may be possible to model this decay time as a disk with self-gravity driving the viscosity. Detailed numerical calculations of self-gravitating disks support the contention that the self-gravity torque can be efficient enough to maintain the disk at the edge of instability to self-gravity, and that the relevant physical length scales are small, of order the disk thickness h, in which case a local viscosity formalism can be utilized (e.g., Lodato & Rice 2004).

3.2. *Segment II: Transient Plateau*

$\alpha_{\rm II} \simeq 0.5$ for $10^3 \lesssim t \lesssim 10^4$ s: The isotropic luminosity observed during the plateau 10^{46} erg s^{-1} translates into a mass accretion rate of $\sim 5 \times 10^{-3} M_\odot$ yr^{-1} after applying the corrections given earlier. We argue that the plateau stage occurs when a small amount of material forms a torus at the radius of the progenitor, $\sim 10^{11}$ cm. The similarity solutions discussed earlier apply to accretion disks that have had time to adjust into a quasi-equilibrium profile which is close to steady-state. Therefore in practice there will be a period of adjustment during which time the small amount of gas ($\gtrsim 3 \times 10^{-5} M_\odot$) that once was part of the envelope of the progenitor becomes stretched out due Keplerian shear into an accretion disk. The time dependent calculations of Cannizzo et al. (1990) indicate a flat transient period in the light curve in response to an annulus of material being suddenly introduced near a central mass. An apparent problem with the light curves shown in Cannizzo et al. (1990, see their Fig. 3) is that the transient plateaus shown there have slightly increasing fluxes, whereas the *Swift* XRT plateaus are flat or decaying. The initial conditions for their time dependent calculations were tori with physically ad hoc Gaussian radial profiles, $\Sigma(r) \propto \exp[-(r - r_c)^2/(2w)^2]$, with $w/r_c = 0.5$. Therefore time was required after the calculations started for matter to spread significantly to smaller radii, approach the standard disk profile $\Sigma(r) \propto r^{-3/4}$, and raise the central accretion rate onto the BH. For the present problem, however, it is more likely that one begins with significant amounts of gas at smaller radii. Therefore the accretion rate onto the BH would reach a higher level more quickly, and the light curves would be flat or decaying. Obviously, time-dependent accretion disk calculations for the present problem are desired, were a physically motivated initial $\Sigma(\vec{r}, \vec{v})$ profile available from SN fall-back calculations.

Since our scenario begins to come into play at the beginning of segment II, the accreted masses quoted earlier for segments II through IV must add up to a minimum for our initial disk mass, i.e., about $3.5 \times 10^{-5} M_\odot$. The relation between Σ_0, r_0, and t_0 given in eqn. (45), in combination with the numerical normalization from Cannizzo et al. (1990, see their Fig. 3), can be used to form a scaling for this interval

$$t_0 \simeq 5 \times 10^4 \text{ s } r_{0,\ 11}^{7/3}\ \alpha_{-1}^{-4/3}\ M_{d,\ -4.5}^{-2/3}\ m_{\rm BH,\ 1}^{1/3}. \qquad (59)$$

where $r_{0,\ 11} = r_0/10^{11}$ cm, and $M_{d,\ -4.5} = M_{\rm disk}/10^{-4.5} M_\odot$. We argue that this plateau period corresponds to Zhang et al's phase II.

3.3. *Segment III*

3.3.1. *Standard Disk*

$\alpha_{\rm III} \simeq 1.2$ for $10^4 \lesssim t \lesssim 10^5$ s: This segment corresponds to the standard model for the outer disk for which the solution given earlier applies. Gas left over from the progenitor

envelope at $\sim 10^{11}$ cm has become smeared out and evolved into the radial profile of an accretion disk, and now the classical similarity solution for the decay begins to apply. The disk mass varies as $t^{-3/16}$ so the luminosity, which scales with dM_d/dt, varies as $t^{-19/16} \simeq t^{-1.2}$. For other opacity laws $\kappa = \kappa_0 \rho^a T^b$, Cannizzo, Lee, & Goodman (1990) found $d\log L/d\log t = -(38+18a-4b)/(32+17a-2b)$. This reduces to the electron scattering limit $(-19/16)$ for $a = b = 0$. In the optically thick limit, the decay rate is relatively insensitive to the opacity law. For instance, a Kramer's law $a = 1$, $b = -3.5$, gives a decay rate $d\log L/d\log t = -5/4$.

3.3.2. *Super-Eddington Slim Disk/ADAF-like state*

For GRBs with high rates of accretion in the post fall-back disk, conditions may be so extreme that the standard model is not relevant. Therefore the super-Eddington slim disk must be considered. In section 2.4.2 we present the time dependent solution for such disks, and show that for early times $d\log L/d\log t = -4/3$, which would probably be indistinguishable in the XRT data from the standard disk value $d\log L/d\log t = -19/16$. Kumar, Narayan, & Johnson (2008a; see their sections 3.1 and 3.2) take a different approach in calculating the time dependent evolution of the transient disk. Rather than solving the $\Sigma(r,t)$ evolution equation they prescribe a functional form $\dot{M}(r) \propto r^s$, and then solve for the total disk angular momentum, mass, and outer radius. The motivation for this $\dot{M}(r)$ form is that for "ADAF-like" conditions one expects strong mass outflow driven by a positive Bernoulli constant (Narayan & Yi 1994, 1995). Thus $s = 0$ would represent no mass loss, and $s = 1$ would correspond to a flow in which 90% of the mass is lost from the disk for each inward decade in radius. This technique bypasses the need for a detailed treatment of the $\Sigma(r,t)$ evolution equation and the kinematic viscosity ν. It also ignores any potential transient phase through which the disk might have to evolve, and therefore assumes that the disk goes immediately into its equilibrium state. They derive a luminosity decay law $L_d(t) \propto t^{-4(s+1)/3}$, which reduces to $t^{-4/3}$ for $s = 0$. This agrees with our law for super-Eddington slim disks at early times.

3.4. *Segment IV*

3.4.1. *Irradiation Dominated Disk*

$\alpha_{\rm IV} \simeq 2$ for $t \gtrsim 10^6$ s: Menou, Perna, & Hernquist (2001) consider the evolution of supernova fall-back disks and find that irradiation becomes important at late times $t \gtrsim 10^6$s. Since the radial decrease in irradiation temperature is flatter than that for disk temperature $(r^{-1/2}$ versus $r^{-3/4})$, as the disk mass decreases and the surface densities and temperatures in the outer disk continue to drop, at some point the condition $T_{\rm irr} > T_{\rm viscous}$ will be satisfied, and the standard model similarity solution will be supplanted by the irradiation model solution. Moreover, a strong wind will begin to deplete significantly the disk mass, at a rate that exceeds the local mass flow (Begelman, McKee, & Shields 1983, Begelman & McKee 1983, Shields et al. 1986). Therefore the decay rate will steepen from the standard model value $\alpha \simeq 1.2$. Begelman, McKee, & Shields (1983, see their eqn. [4.2]), derive a characteristic mass loss rate due to a Compton heated wind

$$\dot{M}_{\rm ch} = 4.5 \times 10^{-7}\ M_\odot\ {\rm yr}^{-1}\ \zeta L_{38} \left(\frac{L_{\rm cr}}{L}\right)^{1/3},\quad (60)$$

where ζ is a collection of factors of order unity, and $L_{\rm cr} \simeq 0.03 L_{\rm E}$. Taking a luminosity $L = \epsilon \dot{M}c^2$ gives

$$\dot{M}_{\rm ch} \simeq 2 \times 10^{-3}\ M_\odot\ {\rm yr}^{-1}\ (\epsilon_{-1}\dot{m}_{-2})^{2/3}m_{\rm BH,\,1}^{1/3},\quad (61)$$

which will serve as a strong source of mass depletion in the outer disk.

The time-dependent decay solution for the wind-driven phase presented in section 2.4.3 is not complete because it does not include the effect of mass decrease on $\Sigma(r,t)$. Also, the decay law, $\alpha_{\rm IV} = 4/3$, is the same as the early-time solution for the super-Eddington slim disk, therefore could not account for the steepening decay for segment IV. The generalized Kumar et al. (2008a) decay solution in the presence of a disk wind, $L_d(t) \propto t^{-4(1+s)/3}$, provides more insight into the potential effect of a wind. The fact that when a segment IV is observed it has a steeper slope than segment III suggests that if there are ADAF-like conditions in the disk early on, mass loss is not significant since the observed decay rate agrees with theoretical one if $s \simeq 0$. Since the ADAF-like state is supposed to be driven by a positive Bernoulli constant, as the disk mass drains and physical conditions within the disk become less extreme, one would not expect for mass loss to become stronger if the positive Bernoulli constant were the only force driving mass loss. However, in the picture of Menou, Perna, & Hernquist (2001), in which irradiation becomes important at later times as a strong agent in driving a wind, a power law $\dot{m}(r) \propto r^s$ to characterize the variation of mass flow within the disk in the presence of strong evaporation may become relevant. The steeper decay law in segment IV would then indicate a significant non-zero s value: for example a nominal value $s \simeq 0.5$ would be required to obtain $L_d(t) \propto t^{-2}$.

3.4.2. *Super-Eddington Slim Disk, late time solution*

In section 2.4.2 we found that for the time dependent super-Eddington slim disk, the disk mass for $t \gtrsim 0.1(\alpha\Omega_0)^{-1}$ varies as $M_d(t) \propto t^{-4/3}$, and therefore $L_d(t) \propto t^{-7/3}$. This is close to the $\alpha_{\rm IV} \simeq 2$ from Zhang et al. (2006) and suggests another possibility for the late time decay. In section 2.3.1 we presented the standard scalings for usual accretion disk with $\nu \propto P_{\rm gas}$ and $\kappa = \kappa_{\rm es}$. A look at the various self-consistency tests showed that most of them were at least marginally validated for conditions expected in the outer disk during segment II. However, the range of isotropic-equivalent luminosities for segment II (Dainotti et al. 2008) can range up to ~ 2 orders of magnitude greater than that adopted in section 2.3.1, which would place an uncomfortable strain on the standard model. For GRBs with outer disks at such extreme conditions that the standard model does not apply, the super-Eddington slim disk maybe a better description. The range in $L_{\rm II}$ values shown in Dainotti et al. (2008) appear to show an intrinsic scatter, therefore there may be GRBs for which the standard model does apply at late times (low $L_{\rm II}$), and others for which the slim disk model is required (high $L_{\rm II}$). One prediction of this idea would be that intrinsically brighter bursts would be more likely to exhibit a segment IV, with its steeper decay. However, for the fainter bursts one would not be able to follow the late-time decay to as low a flux level, and therefore it might be difficult to make a definitive observational statement about the presence of a segment IV.

3.5. *Mass supply: Viscous accretion vs. Fall-back*

Kumar et al. (2008b) present and discuss the criteria for determining whether viscous accretion or fall-back will be the primary supply mechanism feeding mass into the central engine. Both processes will influence the light curve, but the one with the longer time scale is likely to have the dominant effect. After the SN has occurred, the fall-back time for an element of gas in the progenitor envelope to fall from radius r to the BH is roughly the free-fall time $t_{fb} \sim 2(r^3/GM_{BH})^{1/2}$. (This ignores any residual pressure support during the collapse, and other effects such as a wind from the accretion disk and a shock originating near the BH during its formation.) Inverting this expression gives the radius in the star expected to be accreting at a given time t after the SN occurs, $r_{10} \simeq 1.5 t_2^{2/3} m_{BH, 1}^{1/3}$, where $t_2 = t/100$ s. The specific angular momentum $j_{*,18} = 3.6 m_{BH, 1}^{1/2} r_{10}^{1/2} f_\Omega(r)$, where $j_{*,18}$ is in units of 10^{18} cm^2 s^{-1}, and $f_\Omega(r)$ is the local angular velocity of a gas at radius r in the progenitor, in terms of the Keplerian value Ω_K. After the SN explosion, gas which ends up being trapped in the potential well of the BH will fall inward to the point where it hits its angular momentum barrier, determined by $f_\Omega(r)$. This viscous accretion time scale $t_{acc} \simeq (r/h)^2 (\alpha \Omega_K [r_{circ}])^{-1} \approx 2\alpha^{-1} \Omega_K^{-1}(r_{circ})$ (since $h/r \simeq 1$), where r_{circ} is the circularization radius $\sim j_*^2/(GM_{BH})$. This line of reasoning leads to eqn. [4] of Kumar et al. (2008b),

$$t_{acc}/t_{fb} \simeq 10\alpha_{-1}^{-1} f_\Omega^3(r). \qquad (62)$$

Kumar et al. (2008b) note that this relation implies the accretion time will be shorter than the fall-back time, and therefore subordinate as a mass supply mechanism, for $f_\Omega(r) \lesssim 0.4$. They find that the steep decay segment (I) would be possible only if the disk can adjust rapidly to a decrease in $\dot{M}_{fb}$, and use this consideration to place an upper limit on the rotation speed in the core (on the assumption that segment I is due to fall-back of the progenitor core). Their approach is strengthened by our finding that all plausible disk states give decay rates with power laws $\lesssim 2$, too shallow to explain segment I.

At early times before the disk has had a significant opportunity to spread, the fundamental physical considerations presented by Kumar et al. (2008b) seem well-motivated. At later times, however, the increasing viscous time scale associated with the outer disk edge, and the maintenance of a causal coupling to smaller radii, via angular momentum transport, begin to introduce a significant correction factor that must be taken into account in eqn. (62). It is important to note that implicit in the derivation of eqn. (62) is that the radius appearing in the fall-back time and the viscous time are the same. However, the spread of the outer disk edge introduces a strong nonlocality: instead of taking $t_{acc} \propto \alpha^{-1} \Omega_K^{-1}(r_{circ})$ one should more properly consider $\alpha^{-1} \Omega_K^{-1}(r_{disk, outer})$. Since t_{acc} varies as $r^{3/2}$, this introduces a correction factor $(r_{disk, outer}/r_{circ})^{3/2}$ into eqn. (62). Taking a fiducial spreading rate $(r/r_0) = (t/t_0)^{3/8}$ as in the standard solution, and adopting typical numbers for times separating the different segments, $t_{I/II} \simeq 10^3$s, $t_{II/III} \simeq 5 \times 10^4$s, and $t_{III/IV} \simeq 3 \times 10^6$s, this implies an increase over the locally defined (i.e., at r_{circ}) accretion time scale by a factor ~ 8 at $t_{II/III}$ and ~ 90 at $t_{III/IV}$, respectively (stemming from increases of $r_{disk, outer}$ by a factor 4 from $t_{I/II}$ to $t_{II/III}$, and by a factor 20 from $t_{I/II}$ to $t_{III/IV}$). The faster rate of expansion calculated by Kumar et al. (2008a), $(r/r_0) = (t/t_0)^{2/3}$, would give larger correction factors. Also, these factors are

actually lower limits because they only take into account the expansion of the disk relative to $t_{I/II}$. The disk expansion enhances the effect of the accretion supply with respect to the mass supply by prolonging t_{acc}, and also facilitates an understanding of why the steepest decay (segment I) must occur at the earliest time possible, before the significant outward movement in $r_{disk, outer}$ has enforced $t_{acc} >> t_{fb}$.

Kumar et al. (2008b) present examples of 4 *Swift* GRBs for which $\alpha_{III} \simeq 4 - 6$, much steeper than in the standard Zhang et al. (2006) picture $\alpha_{III} \simeq 1.2$. For these rare bursts the Kumar et al. fall-back scenario may well provide a better description than our viscous accretion disk scenario.

4. DISCUSSION

The overarching question behind this study is the following: Is the very long term ($t \gtrsim 10^6$s) decay seen in the X-ray flux from GRBs due to the deceleration of a relativistic jet, or to a decreasing mass supply onto the central engine? We argue in favor of the latter. We have presented a general scenario for understanding the long term evolution, in particular the four power law decay segments found through *Swift* XRT observations. The basic idea relies on the fact that the ever-expanding outer edge maintains a causal connection through the intervening radii all the way to the inner disk, given the coupling of the viscosity mechanism to the local shear in the disk. In more basic terms, the mass of the accretion disk decreases as a power law in time, resulting in a decrease in mass accretion rate at the inner edge.

The overall evolution is as follows:

(I) The initial steep decay phase arises from the dynamical fall-back of $\sim 0.1 M_\odot$ of material into the vicinity of the BH (Kumar, Narayan, & Johnson 2008ab). Kumar et al. 2008b show by comparing the viscous and fall-back times in the early stages of fall-back that $t_{acc} << t_{fb}$. The disk therefore responds quickly to the steeply decreasing, externally imposed mass supply from the progenitor core. This scenario is only possible at early times before expansion of the outer accretion disk causes $t_{acc} > t_{fb}$. An alternative but perhaps less likely possibility for the steep decay involves completely different physics (Pe'er et al.[5] 2006).

(II) The initial establishment of the disk leads to a brief transient phase during which calculations indicate a flat light curve. This corresponds to the viscous smearing and spreading of gas left over from the progenitor envelope into an accretion disk (Cannizzo et al. 1990), which we take to lie at roughly the progenitor radius $\sim 10^{11}$ cm. The dynamical time scale there $\Omega_K^{-1} \sim 10^3$s is toward the lower range of observed plateau durations (Dainotti et al. 2008, se their Figs. 1 and 2), and our scaling for the transient period following the arrival of material to establish the accretion disk is in line with the duration of the plateau phase seen in some of the XRT light curves.

The plateau phase has been ascribed by previous workers to continued activity of the central engine, or to the accretion disk having low value of the Shakura-Sunyaev α parameter (e.g., Kumar, Narayan, & Johnson 2008a; although in their final analysis they downgrade this possibility). Given the apparent robustness of the non-linear saturation limit of the viscosity parameter in the MRI process (Beckwith, Hawley, &

---

[5] Their explanation, which involves a hot cocoon with modest Lorentz factor and a nearly thermal spectrum, may be refuted by *Swift* observations showing that the GRB prompt emission joins smoothly to segment I — an unlikely coincidence given that the hot cocoon represents an independent physical component.

Krolik 2008), however, we also view the small α explanation as unlikely. Kumar, Narayan, & Johnson (2008a) view as a more plausible explanation continued fall-back onto the central BH. Kumar, Narayan, & Johnson (2008b; see their Fig. 2) present conditions for the core/envelope density structure of the progenitor that would be required to obtain the plateau (as well as the steeper segments - I and III). In the previous section we showed how the spreading of the outer disk enhances the effective viscous accretion time, relative to the fall-back time, and ensures that viscous accretion will become increasingly dominant as the outer disk expands significantly beyond what had been the radius of the progenitor.

(III) After the transient period, the outer disk becomes describable using the standard formalism ($t^{-1.2}$ decay) or an advective formalism ($t^{-1.3}$ decay). The continued high rate of accretion substantially depletes the mass of the disk. The inner disk is still not only substantially super-Eddington (by a factor $\sim 10^5 - 10^7$) but also potentially degenerate due to the very high densities (e.g., Narayan, Piran, & Kumar 2001, Kohri & Mineshige 2002, Kohri, Narayan, & Piran 2005, Chen & Beloborodov 2007, Ohsuga & Mineshige 2007).

(IV) At some point the outer disk may become not only radiation dominated, but also subject to a substantial Compton driven wind, leading to an increase in the decay rate. If the rate of mass flow within the body of the disk can be characterized $\dot{M}(r) \propto r^s$ as in Kumar et al. (2008a), then their decay solution $L_d(t) \propto t^{-4(1+s)/3}$ would provide a good fit for $s \approx 0.5$ regardless of whether the disk was standard or advective. Alternatively, our late time super-Eddington slim-disk solution $L_d(t) \propto t^{-7/3}$ may apply at this time.

Depending on details such as the initial mass of the disk, states (II) and (IV) may or may not become manifest in the long term light curve.

The current paradigm for the long term GRB light curves attributes changes seen in the decay properties to variations (i.e., a decrease) in the bulk Lorentz flow of a jet of material expelled from the central engine as it collides with and interacts with circumstellar material. We argue that a strong jet is established almost immediately after the GRB prompt emission, and the subsequent decay properties of the light curve are set by a dwindling mass supply due to the long term decrease in Σ at all radii. The decay law obtained by Kumar et al. (2008a) in which $L_X \propto t^{-4(s+1)/3}$, where the mass loss rate from the disk varies as r^s, allows for a range of decay between $t^{-4/3}$ and $t^{-8/3}$. The steeper decay, as an explanation for segment III, seems to be excluded by the data (e.g., Ghisellini et al. 2009, see their Fig. 16). If the slim disk/ADAF picture proves to be a valid description of the outer disk, the observed segment III decay rate would appear to argue against a strongly varying mass loss rate with radius. Also, the potential bimodality in decay rate with time found in section 2.4.2 for the slim disk state, $t^{-4/3}$ for early times and $t^{-7/3}$ for late times, might play a role in the III/IV transition. The dividing point lies at $\sim 10^3 \text{s} \, r_{0,11}^{3/2} m_{BH,1}^{-1/2} \alpha_{-1}^{-1}$, so for this to work the disk would have to have expanded to $\gtrsim 10^{12}$ cm to account for the long time scale $\sim 10^4 - 10^5$s of the III/IV transition. Alternatively, the onset of a strong wind at late times, driven by irradiation, may force s to increase from 0 to ~ 0.5, thereby steepening the decay in segment IV.

In addition to our alternative explanation for the plateau seen in some of the XRT light curves, there is also an issue raised by the high-latitude emission model (Kumar & Panaitescu 2000). In this model, after the mechanism responsible for producing X-ray emission ceases, an observer along the central jet axis sees continued emission as photons from increasingly off-axis lines of sight continue to arrive. For uniform surface brightness, an intrinsic spectrum $\nu^{-\beta}$ produces a power law decay in time $t^{-\alpha}$, where $\alpha = \beta + 2$. This prediction was tested by O'Brien et al. (2006, see their Fig. 4) for the initial decay segment (Zhang et al's I) using a large sample of *Swift* GRBs. Instead of $\alpha \simeq \beta + 2$, they found a scatterplot in α versus β. Thus the standard model also seems problematic for decay segment I as regards the temporal/spectral evolution, although more recent work on the high-latitude "curvature effect" has been promising (Zhang et al. 2007, 2009).

5. IMPLICATIONS

Eqn. (1) of Sari, Piran, & Halpern (1999) has proven of great use to observers insofar as it relates observable quantities, namely jet break time, redshift, and GRB fluence, to a beaming angle (assuming a density of the circumstellar medium). The outline of the theory we present is not yet sufficiently developed to build a complex formalism. Simple statements can still be made, however. Our eqn. (59) gives an approximate scaling for the time of the segment II/III transition. If the luminosity of the plateau scales roughly with the mass accumulated during fall-back that supplies the transient disk associated with the plateau (segment II) in our model, then eqn. (59) predicts an inverse scaling between $L_{X,II}$ and $t_{II, III}$, namely $L_{X,II} \propto t_{II, III}^{-3/2}$. (This ignores the r_0 scaling, however.) An inverse correlation is observed in the data, but appears less steep ($L_{X,II} \propto t_{II, III}^{-0.8}$) than our prediction (Dainotti, Cardone, & Capozziello 2008; see their Figs. 1 and 2).

The Kumar et al. (2008a) decay law with mass loss from the disk, $L_d(t) \propto t^{-4(1+s)/3}$, is consistent with our early time decay law for the super-Eddington slim disk, and with the observed value $\alpha_{III} \simeq 1.2$, for $s = 0$. It is also close to the decay law for standard disks, $L_d(t) \propto t^{-19/16}$. This appears to indicate that for very high $\dot{M}$ disks where the standard model is not applicable during segments II and III, if an ADAF-like state is correct, then mass loss must be minimal (i.e., $s \simeq 0$, or $\dot{M}(r) \simeq$ constant). The steepening then associated with segment IV could either be due to the onset of significant evaporation, e.g., $s \simeq 0.5$ would be sufficient, or the late time super-Eddington slim disk law $L_d(t) \propto t^{-7/3}$.

If our model has some merit, then a revision in current thinking would be needed. First, there may not be a standard GRB energy reservoir as in Frail et al. (2001). Also, for the jet to respond quickly to whatever conditions prevail at the central engine (i.e., accretion rate), it may need to be a light-weight jet with a low degree of baryon loading. It may be a Poynting-flux dominated jet as in the model of Lyutikov & Blandford (2003). The deceleration experienced by such a jet would tend to be less, for a given energy flux. The previous estimates of the circumstellar density field $n(r)$ would need to be revised. Conversely, the jet may be baryon-loaded during the steep decay segment (segment I) which appears to be too steep to be covered within an accretion disk formalism. The spectral evolution observed during this phase may be difficult to account for with a purely EM jet (O'Brien et al. 2006; Pe'er et al. 2006). There may also be some baryon loading during the rest of the decay, but the density of the circumstellar medium would need to be less than previously thought, so that deceleration would be minimal.

In this work we have implicitly assumed that the X-ray light curve represents the bulk of the radiated jet energy. Therefore our model runs into the same difficulty as the standard model in accounting for why the breaks seen at other wavelengths do not follow the X-ray. The physical emission mechanisms must differ across different wavebands, which could also potentially mitigate one of the criticisms of the standard model. One idea currently being discussed is that, within a given GRB there can co-exist jets with different opening angles and different physical conditions, each of which can contribute preferentially to emission in different wavebands. If the opening angles are considerably different, this could lead to different break times (e.g., Racusin et al., 2008). Our simple model is not yet developed enough to make any predictions on the relative rates of decay at different wavelengths.

There are other important issues to consider, such as the formation and stability of an accretion disk in the middle of a supernova. Enough material would have to be evacuated from the vicinity of the disk near the BH at early times to permit the disk to survive the expected shocks and radiation of the explosion. Also, if the BH acquires a kick velocity $v_{\rm kick}$ during the initial explosion, this velocity would have to be small enough so that the accretion disk was not left behind. (A simple consideration of the binding energy shows that matter in the disk with $v_{\rm orbit} = 1155$ km s^{-1} $m_{\rm BH,1}^{1/2}$ $r_{11}^{-1/2} > v_{\rm kick}$, where $v_{\rm kick} \simeq 100 - 300$ km s^{-1}, should remain bound to the BH.) Finally, the jet issuing from the BH would have to be powerful enough to punch through the veil of material comprising the ejecta, and to maintain an open channel for $\gtrsim 10^6$s. If the jet is primarily electromagnetic as opposed to baryon-loaded, the open EM field lines may help in maintaining a clear path for the jet beam.

Recently various workers have proposed a simple way for obtaining the flat decay associated with segment II. Implicit in our work and that of others such as Kumar et al. (2008ab) is that the start of the prompt emission is the relevant start time for all the other emission — X-ray, optical, and radio. It is possible that the physical mechanism responsible for producing the X-rays actually commences $\sim 10^4 - 10^5$s before the prompt emission, so that the flat appearance of segment II is merely due to having an incorrect start time (Yamazaki 2009; Liang et al. 2009). Yamazaki (2009) plots four examples of GRBs for which a shifting of the start time for the X-ray decay produces a good fit for the plateau, after having optimized the decay for segment III. One can however find other examples of GRBs for which there is a gradual decay in segment II that is not well-fit by simply shifting the start time, therefore this explanation may not work for all GRBs. Also, it remains unclear as to how the X-ray emission could begin significantly before the GRB, which presumably marks the moment of explosion of the progenitor and formation of the BH.

6. CONCLUSION

We present a new paradigm for understanding the long-term behavior of GRBs, as inferred primarily through *Swift* XRT observations. We argue that the four power law segments into which the long term XRT light curves can be divided can be explained by the time dependent evolution of the external accretion disk. The initial, steep period of decay happens before the external accretion disk has been established and therefore is beyond our scope (although a self-gravitating disk remains a possibility). Simple estimates of the accretion and fall-back time scales $t_{\rm acc}$ and $t_{\rm fb}$ indicate that fall-back will be dominant at the earliest times. Therefore the fact that segment I has the steepest slope, too steep to be accounted for by the disk models we study, strengthens the picture advocated in Kumar et al. (2008b) in which the direct fall-back of the progenitor core leads to segment I. After the initial evolution, expansion of the outer disk edge enforces $t_{\rm acc} > t_{\rm fb}$ so that accretion is dominant. We ascribe the subsequent flattening in the GRB light curves to a period of viscous re-adjustment in the accretion disk formed out of the gas elements from the progenitor envelope that remain bound to the BH and end up at their specific angular momentum radii after the hypernova explosion. The following steepening corresponds to the similarity solution for the decay of a standard disk or advective disk at the largest radii, and the further slight steepening at later times could be due to the additional mass depletion from a strong wind, or in some cases to the late time evolution of a super-Eddington slim disk.

REFERENCES

Abramowicz, M. A., Czerny, B., Lasota, J.-P., & Szuszkiewicz, E. 1988, ApJ, 332, 646
Balbus, S. A., & Hawley, J. F. 1998, Rev Mod Phys, 70, 1
Balbus, S. A., & Papaloizou, J. C. B. 1999, ApJ, 521, 650
Beckwith, K., Hawley, J. F., & Krolik, J. H. 2008, ApJ, 678, 1180
Begelman, M. C., King, A. R., & Pringle, J. E. 2006, MNRAS, 370, 399
Begelman, M. C., & McKee, C. F. 1983, ApJ, 271, 89
Begelman, M. C., McKee, C. F., & Shields, G. A. 1983, ApJ, 271, 70
Blandford, R. D., & Znajek, R. L. 1977, MNRAS, 179, 433
Blustin, A. J., et al. 2006, ApJ, 637, 901
Burrows, D. N., et al. 2005, Science, 309, 1833
Cannizzo, J. K. 1997, ApJ, 482, 178
Cannizzo, J. K., Lee, H. M., & Goodman, J. 1990, ApJ, 351, 38
Cannizzo, J. K., & Reiff, C. M. 1992, ApJ, 385, 87
Chen, W.-X., & Beloborodov, A. M. 2007, ApJ, 657, 383
Chen, X., Abramowicz, M. A., Lasota, J.-P., Narayan, R., & Yi, I. 1995, ApJ, 443, L61
Curran, P. A., et al. 2007, MNRAS, 381, L65
Dai, X., Halpern, J. P., Morgan, N. D., Armstrong, E., Mirabal, N., Haislip, J. B., Reichart, D. E., & Stanek, K. Z. 2007, ApJ, 658, 509

Dainotti, M. G., Cardone, V. F., & Capozziello, S. 2008, MNRAS, 391, L79
Done, C., Gierliński, M., & Kubota, A. 2007, Astr & Astrophys Rev, 15, 1
Frail, D. A., et al. 2001, ApJ, 562, L55
Fryer, C. L., Colgate, S. A., & Pinto, P. A. 1999, ApJ, 511, 885
Gehrels, N., et al. 2004, ApJ, 611, 1005
Gehrels, N., Ramirez-Ruiz, E., & Fox, D. B. 2009, ARAA, in press
Ghisellini, G., Nardini, M., Ghirlanda, G., & Celotti, A. 2009, MNRAS, 393, 253
Ghosh, P., & Abramowicz, M. A. 1997, MNRAS, 292, 887
Grupe, D., et al. 2007, ApJ, 662, 443
Hirose, S., Krolik, J. H., & Blaes, O. 2009, ApJ, 691, 16
Kato, S., Fukue, J., & Mineshige, S. 1998, Black-Hole Accretion Disks (Kyoto Univ. Press; Kyoto)
Kawanaka, N., & Mineshige, S. 2007, ApJ, 662, 1156
Kocevski, D., & Butler, N. 2008, ApJ, 680, 531
Kohri, K., & Mineshige, S. 2002, ApJ, 577, 311
Kohri, K., Narayan, R., & Piran, T. 2005, ApJ, 629, 341
Krolik, J. H., Hawley, J. F., & Hirose, S. 2007, Rev. Mex. A. A., 27, 1
Kumar, P., Narayan, R., & Johnson, J. L. 2008a, MNRAS, 388, 1729
Kumar, P., Narayan, R., & Johnson, J. L. 2008b, Science, 321, 376

Kumar, P., & Panaitescu, A. 2000, ApJ, 541, L51
Lazzati, D., Perna, R., & Begelman, M. C. 2008, MNRAS, 388, L15
Liang, E.-W., Lü, H.-J., Zhang, B.-B., & Zhang, B. 2009, astro-ph/0902.3504
Liang, E.-W., Racusin, J. L., Zhang, B., Zhang, B.-B., & Burrows, D. N.
    2008, ApJ, 675, 528
Lightman, A. P., & Eardley, D. M. 1974, ApJ, 187, L1
Livio, M., Ogilvie, G. I., & Pringle, J. E. 1999, ApJ, 512, 100
Lodato, G., & Rice, W. K. M. 2004, MNRAS, 351, 630
Lyutikov, M., & Blandford, R. D. 2003, astro-ph/0312347
MacFadyen, A. I. & Woosley, S. E. 1999, ApJ, 524, 262
McKinney, J. C., & Narayan, R. 2007a, MNRAS, 375, 513
McKinney, J. C., & Narayan, R. 2007b, MNRAS, 375, 531
Menou, K., Perna, R., & Hernquist, L. 2001, ApJ, 559, 1032
Nagataki, S., Takahashi, R., Mizuta, A., & Takiwaki, T. 2007, ApJ, 659, 512
Narayan, R., Piran, T., & Kumar, P. 2001, ApJ, 557, 949
Narayan, R., Yi, I. 1994, ApJ, 428, L13
Narayan, R., Yi, I. 1995, ApJ, 444, 231
Nousek, J. A., et al. 2006, ApJ, 642, 389
Oates, S. R., et. al. 2007, MNRAS, 380, 270
O'Brien, P. T., et al. 2006, ApJ, 647, 1213
Ohsuga, K., & Mineshige, S. 2007, ApJ, 670, 1283
Pe'er, A., Mészáros, P., & Rees, M. J. 2006, ApJ, 652, 482
Perna, R., Armitage, P. J., & Zhang, B. 2006, ApJ, 636, L29

Pringle, J. E. 1974, PhD thesis, Univ. of Cambridge
Pringle, J. E. 1991, MNRAS, 248, 754
Racusin, J. L., et al. 2008, Nature, 455, 183
Rhoads, J. E. 1997, ApJ, 487, L1
Rhoads, J. E. 1999, ApJ, 525, 737
Sakamoto, T., et al. 2008, ApJS, 175, 179
Sari, R., Piran, T., & Halpern, J. P. 1999, ApJ, 519, L17
Shakura, N. I., & Sunyaev, R. A. 1973, A&A, 24, 337
Shields, G. A., McKee, C. F., Lin, D. N. C., & Begelman, M. C. 1986, ApJ,
    306, 90
Smak, J. 1984, Acta Astr., 34, 161
Stanek, K. Z., et al. 2007, ApJ, 654, L21
Willingale, R., et al. 2007, ApJ, 662, 1093
Woosley, S. E. 1993, ApJ, 405, 273
Woosley, S. E., & Bloom, J. S. 2006, ARAA, 44, 507
Yamazaki, R. 2009, ApJ, 690, L118
Yuan, F., Ma, R., & Narayan, R. 2008, ApJ, 679, 984
Zhang, B., et al. 2006, ApJ, 642, 354
Zhang, B.-B., E.-W., Liang, & Zhang, B. 2007, ApJ, 666, 1002
Zhang, B.-B., Zhang, B., E.-W., Liang, & Wang, X.-Y. 2009, ApJ, 690, L10